로켓 방화벽용 열경화성 복합재의 거동해석

이 선 표* · 이 정 윤*

Analysis of Thermo Chemically Decomposing Composites for Rocket Thermal Insulators

Sunpyo Lee* · Jung Youn Lee*

ABSTRACT

A theory for time-dependent, high temperature ablation of poroelastic carbon composite insulators is applied using finite element methods to determine material properties fron experimental data. The theory contains important revisions to that in Lee, Salamon and Sullivan[1] by making a sharp distinction between Biots constants and permeability and setting both to analytical functions of porosity. The finite element program and material modeling has been modified to (1) more closely adhere to porous-material theory, (2) include a newly discovered analytical simplification and (3) refine the material property descriptions. Application tc experimental problems and comparisons with data permit determination of Biots constants and permeability and their evolution with respect to matrix decomposition and clearly show how material parameters affect the material response, e.g., amplitude and the location of peaks with respect to temperature. In particular, the response is very sensitive to permeability and dominated by it.

초 록

다공성 카본 페놀릭 복합재의 재료상수를 실험데이터로부터 결정하기 위하여 시간의존 이론과 유한요소법을 적용하였다. 이 이론은 Biot 의 상수와 투과율 사이의 관계를 다공성의 함수로 사용하여 기존의 Lee, Salamon, Sullivan[1]의 논문을 수정하였다. 수정된 유한요소 프로그램과 재료의 모델링은 (1) 다공성 재료 이론에 더 충실하고 (2) 새롭게 발견된 해석적 단순함을 포함하고 (3) 재료의 성질을 더욱 정확하게 기술하였다. 실험 데이터에 대한 적용과 비교는 어떻게 재료의 파라미터들이 재료의 응답 즉 온도에 따르는 압력의 크기와 최대치의 위치 지배되는지 명백하게 나타낸다. 특별히 응답이 투과율에 매우 민감하게 나타났다.

* 경기대학교 전자기계공학부

로켓 방화벽용 열경화성 복합재의 거동해석

이 선 표* · 이 정 윤*

Analysis of Thermo Chemically Decomposing Composites for Rocket Thermal Insulators

Sunpyo Lee* · Jung Youn Lee*

ABSTRACT

A theory for time-dependent, high temperature ablation of poroelastic carbon composite insulators is applied using finite element methods to determine material properties from experimental data. The theory contains important revisions to that in Lee, Salamon and Sullivan[1] by making a sharp distinction between Biots constants and permeability and setting both to analytical functions of porosity. The finite element program and material modeling has been modified to (1) more closely adhere to porous-material theory, (2) include a newly discovered analytical simplification and (3) refine the material property descriptions. Application to experimental problems and comparisons with data permit determination of Biots constants and permeability and their evolution with respect to matrix decomposition and clearly show how material parameters affect the material response, e.g., amplitude and the location of peaks with respect to temperature. In particular, the response is very sensitive to permeability and dominated by it.

초 록

다공성 카본 페놀릭 복합재의 재료상수를 실험데이터로부터 결정하기 위하여 시간의존 이론과 유한요소법을 적용하였다. 이 이론은 Biot 의 상수와 투과율 사이의 관계를 다공성의 함수로 사용하여 기존의 Lee, Salamon, Sullivan[1]의 논문을 수정하였다. 수정된 유한요소 프로그램과 재료의 모델링은 (1) 다공성 재료 이론에 더 충실하고 (2) 새롭게 발견된 해석적 단순함을 포함하고 (3) 재료의 성질을 더욱 정확하게 기술하였다. 실험 데이터에 대한 적용과 비교는 어떻게 재료의 파라미터들이 재료의 응답 즉 온도에 따르는 압력의 크기와 최대치의 위치 지배되는지 명백하게 나타낸다. 특별히 응답이 투과율에 매우 민감하게 나타났다.

* 경기대학교 전자기계공학부

NOMENCLATURE

C thermal capacitance matrix
C_p heat capacity
E_{ij} moduli of elasticity
$\boldsymbol{K}$ finite element stiffness matrix
c_1 degree of char
$\boldsymbol{k}$ permeability matrix
p pore pressure
α_i Biots constants
β_i thermal expansion coefficients of solid
ϕ porosity
$\boldsymbol{\kappa}$ thermal conductivity matrix
σ_i total stresses

1. INTRODUCTION

Carbon phenolic composites are thermal insulation materials used to protect rocket nozzle structures from the heat of rocket fuel combustion which flows into the insulation. Key to this process is the thermally-activated decomposition of the phenolic matrix into gases which convect heat away from the structure as they escape through growing pore channels in the decomposing material and carbon fiber skeleton and exit into the rocket exhaust. Initiating at the exhaust surface, the skeleton, known as the char layer, advances into the material, but lags the thermal front. Problems arise when the gases are generated faster than the growth of pore channels can accommodate their flow, hence pore pressures increase to a level which can cause material failure. The failure treated here is cross-ply delamination.

Numerical simulations of decomposition of carbon phenolic composites have been reported by Sullivan and Salamon [2],[3], Weiler [4], Lee, Salamon and Sullivan [1] and Wu and Katsube [5] with a focus on developing a model and simulation code and verifying these against experimental data, primarily that reported by Stokes [6]. All are based upon Biots poroelasticity theory[7] and were reasonably successful. Lee [8] pushed the analysis further. He developed a two-dimensional, axisymmetric finite element code to model a section of rocket engine insulation and structure and used it to simulate a cowl region failure. Ganesan [9] followed suit and developed a one-dimensional code to solve the same problem; a unique feature of his work is an analytical formulation for the pore pressure-to-stress coupling parameter. Lee's results matched the location of an actual failure discovered in a spent space shuttle engine, but Ganesan did not. Subsequently an error was discovered in Lees boundary conditions.

In this paper we revisit the problem and bring to bear new information. Based upon a study by Fabre and Gustkewicz[10], an empirical function for Biots[7] constants in terms of porosity of the material is employed. Moreover building upon Biots[7] form for permeability in terms of porosity, we construct a function for it in terms of open porosity. These functions depend upon porosity and open porosity, respectively, as each varies from the virgin to the charred state of the material. Hence each quantity has a very distinct physical basis. With other modest revisions to the theory of Lee, Salamon and Sullivan[1], the simulations are run using a version of Lees code [8] which

has been modified to adhere to the theory include a newly discovered simplification to the finite element formulation, and employ refined material property descriptions. We study the sensitivities of behavior with respect to the permeability and Biots constants over the evolution of pore growth from closed to open state. The results allow determination of material properties by comparison with Stokes tests[6].

2. AXISYMMETRIC THEORY

The theory in axisymmetric coordinates with radius r and axis z, is built upon Lee, Salamon and Sullivans[1] formulation for the momentum, gas transfer and energy balance differential equations. Here only pertinent portions are recalled, but revisions are explicitly denoted.

2.1 Momentum

The momentum equations, ignoring inertia and written in terms of the total stress, are

$$\frac{\partial \sigma_1}{\partial r}+\frac{\partial \sigma_5}{\partial r}+\frac{1}{r}(\sigma_1-\sigma_2)=0$$
$$\frac{\partial \sigma_5}{\partial r}+\frac{\partial \sigma_3}{\partial r}+\frac{1}{r}\sigma_5=0 \qquad (1)$$

where the reduced notation $1\equiv rr$, $2\equiv\theta\theta$, $3\equiv zz$, $4\equiv\theta z$, $5\equiv rz$ and $6\equiv r\theta$ is used. The constitutive relations, which include a temperature differential T and a pore pressure p generated by gas, are

$$\sigma_i=E_{ij}(e_j-\beta_j\Delta T)-p\alpha_i \quad (i=1,2,3,5;\ j\ \textit{summed through}\ 6) \qquad (2)$$
$$\sigma_4=E_{44}e_4+E_{46}e_6\ ,\ \sigma_6=E_{46}e_4+E_{66}e_6$$

where e_i are the usual linear total strain components in terms of displacements u, w in the r, z directions. E_{ij} are the elastic moduli, β_i the coefficients of thermal expansion acting upon temperature change ΔT and α_i the Biot pressure-stress coupling factors, generally referred to as Biots constants.

2.2 Gas Transfer

The gas transfer equation is

$$+\rho_g\frac{\partial}{\partial t}\left[\alpha_1\frac{\partial u}{\partial r}+\alpha_2\frac{u}{r}+\alpha_1\frac{\partial w}{\partial z}+\alpha_5\left(\frac{\partial w}{\partial r}+\frac{\partial u}{\partial z}\right)\right]$$
$$-\rho_\mu(\alpha_1\beta_1+\alpha_2\beta_2+\alpha_3\beta_3+\alpha_5\beta_5+\phi\beta_g)\frac{\partial T}{\partial t}$$
$$+\frac{\rho_g}{r}\frac{\partial}{\partial r}\left[r\left(\frac{k_1}{\mu}\frac{\partial p}{\partial r}+\frac{k_5}{\mu}\frac{\partial p}{\partial z}\right)\right]$$
$$+\rho_\mu\frac{\partial}{\partial z}\left(\frac{k_5}{\mu}\frac{\partial p}{\partial r}+\frac{k_3}{\mu}\frac{\partial p}{\partial z}\right)$$
$$+\frac{\rho_g}{M}\left(\frac{\partial p}{\partial t}\right)+(\rho_{virg}-\rho_{char})\frac{dc_1}{dt}=0 \qquad (3)$$

where M , ρ_g , k and μ are a material property, gas density, permeability and gas viscosity, respectively. T is temperature of solid and gas (assumed equal), p is pore pressure, c_1 is a measure of charred material, ϕ is the actual porosity as a function of char and t is time. Subscripts virg and char denote virgin and decomposed-to-char (completely charred) material, respectively. The mechanical and thermal properties of dry carbon-phenolic are listed in Appendix. With this information, we determine from the interpolation

$$\phi=c_1\phi_{virg}+(1-c_1)\phi_{char} \qquad (4)$$

where virg is the virgin porosity, char is the charred porosity, and c_1 is the degree of char and has initial value of unity at virgin stage and final value of zero at the completely charred stage.

Pyrolysis gases are treated as ideal and ρ_g is obtained from the ideal gas law where $\rho_g = MW_g p/RT$ is the molecular weight of gas and R is the universal gas constant. Following Sullivan and Salamon[2], the rate of charring is expressed by the Arrhenius kinetic reaction equation

$$(\rho_{virg} - \rho_{char})\frac{dc_1}{dt} = -\sum_{i=1}^{N_r} RF\rho_{virg}(W_{oi} - W_{ci})\ A_i(c_{1i})^{n_i} e^{\left(-\left(\frac{E_a}{RT_a}\right)_i\right)} \quad (5)$$

where N_r is the number of reactions and the various constants involve weight fractions, Arrhenius constants and activation energies for the chemical reactions (Lee, Salamon and Sullivan, [1]). These constants for dry carbon-phenolic are listed in Ref.[1].

Revision 1. The model for determination of permeability with respect to degree of the porosity of the material (Biot [7]) is

$$\phi_k = \phi_{openv} + (\phi_{char} - \phi_{openv})\left(\frac{\phi - \phi_{virg}}{\phi_{char} - \phi_{virg}}\right)$$

$$k = k_{virg}\left(\frac{\phi_k}{\phi_{openv}}\right)^2 \quad (6)$$

where the porosities k, char, openv, virg are open, charred, open virgin and virgin porosity respectively, as shown in Fig. 1. We assume that permeability is dependent upon an open porosity or network of pores, and that porosity at char is open. The open virgin porosity and the permeability of virgin material are determined through simulation. It should be noted that we employ two porosities, but require three: (1) , the actual porosity, is the ratio of volume of pores to

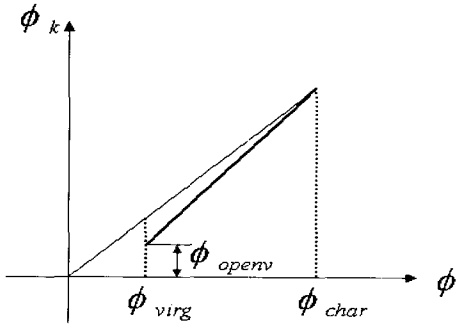

Fig. 1. Open porosity versus actual porosity

the volume of solid which equals the sum of (2) the open porosity, that part of the actual porosity forming a connected, porous network in the material and (3) the closed porosity, the remaining part manifested as isolated pores in the material.

2.3 Energy Balance

The energy balance equation is

$$\rho_{virg}h_R\frac{dc}{dt} - \frac{1}{r}\frac{\partial}{\partial r}\left[r\left(\kappa_1\frac{\partial T}{\partial r} + \kappa_5\frac{\partial r}{\partial z}\right)\right] - \frac{\partial}{\partial z}\left(\kappa_5\frac{\partial T}{\partial r} + \kappa_3\frac{\partial T}{\partial z}\right) - \phi\rho_g(c_p)_g\left(\frac{k_1}{\mu}\frac{\partial p}{\partial r} + \frac{k_5}{\mu}\frac{\partial p}{\partial z}\right)\frac{\partial T}{\partial r} - \phi\rho_g(c_p)_g\left(\frac{k_5}{\mu}\frac{\partial p}{\partial r} + \frac{k_3}{\mu}\frac{\partial p}{\partial z}\right)\frac{\partial T}{\partial z} - \frac{\phi\rho_g(c_p)_g T}{r}\frac{\partial}{\partial r}\left[r\left(\frac{k_1}{\mu}\frac{\partial p}{\partial r} + \frac{k_5}{\mu}\frac{\partial p}{\partial z}\right)\right] - \frac{\phi\rho_g(c_p)_g T}{r}\frac{\partial}{\partial z}\left[r\left(\frac{k_5}{\mu}\frac{\partial p}{\partial r} + \frac{k_3}{\mu}\frac{\partial p}{\partial z}\right)\right] + \frac{\partial}{\partial t}\{[(1-\phi)\rho_s(c_p)_s + \phi\rho_g(c_p)_g]T\} = 0 \quad (7)$$

The last two lines of this equation contain two revisions to Lees theory [8]:

Revision 2. Lees assumption of an ideal gas and its implication that the enthalpy, h = C_pT, C_p the specific heat at constant pressure, is here applied consistently to the leading coefficient in both lines, not just the penultimate line.

Revision 3. Following Ganesan [9], the energy due to enthalpy of the gas is replaced by its effective contribution only within the pore regions of the material, hence ρC_p becomes $\phi\rho C_p$.

2.4 Finite Element Form

The finite element form of these equations is

$$[C]\frac{d}{dt}\{z\}+[K]\{z\}=\{F\} \tag{8}$$

where

$$[C]=\begin{bmatrix} 0 & 0 & 0 & 0 \\ 0 & 0 & 0 & 0 \\ C_{pu} & C_{pw} & C_{pp} & C_{pT} \\ 0 & 0 & 0 & C_{TT} \end{bmatrix}$$

$$[K]=\begin{bmatrix} K_{uu} & K_{uw} & K_{up} & K_{uT} \\ K_{wu} & K_{ww} & K_{wp} & K_{wT} \\ 0 & 0 & K_{pp} & 0 \\ 0 & 0 & K_{Tp} & K_{TT} \end{bmatrix}$$

$$\{F\}=\{\,F_u \;\; F_w \;\; F_p \;\; F_T\}$$

$$\{z\}=\{\,u \;\; w \;\; p \;\; T\} \tag{9}$$

2.5 Material Characterization Results

There are two multi-component poromechanical properties of the material in question: Biots constants α_i and the permeabilities of the material, both of which vary with decomposition of the matrix material. The carbon phenolic composite material is dry FM5055 for which we assume because of lack of data for the applications.

Biots [7] proposed unjacketed experiments to determine ai are prohibitive to carry out. Moreover their analytical determination requires information on the values of the pure solid material compliances as opposed to E_{ij} for the porous solid. Virgin carbon phenolic is assumed to be densely packed with microscopic pores which extends Biot s theory beyond its original intent.

First we assume the $\alpha_i=\alpha$, i = 1, 2, 3 and α_5 = 0

Revision 4. a is determined by: (1) Adopting the Fabre and Gustkiewicz [10] hypothesis which states that the factors must increase with increasing porosity of the material. The following formula for the Biots constants was suggested:

$$\alpha=1-\exp\left[-a\tan\left(\frac{\pi\phi}{2}\right)\right] \tag{10}$$

where a is the coefficient of the porosity, a curve-fitting parameter.

(2) Curve-fitting the simulation results to the restrained thermal growth (RTG) and free thermal expansion (FTE) data due to Stokes [6] to determine a.

2.6 Restrained Thermal Growth Results

The RTG experiment heats a specimen (1.27 cm dia. x 5.72 cm long) at a constant 5.55K/s rate and measures the cross-ply stress to maintain zero strain over a 2.54 cm gage length, Fig. 2. Other details are in the references.

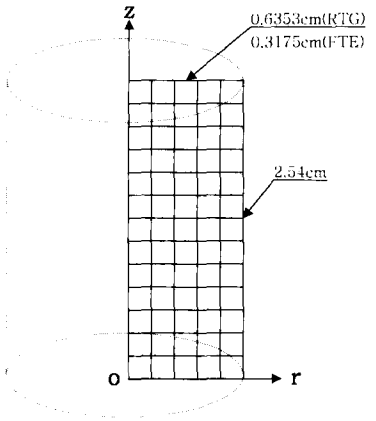

Fig. 2. Illustration of geometry and finite element model for RTG and FTE

2.7 Finite Element Simulation

The simulations employed 160 bilinear, axisymmetric quadrilateral finite elements uniformly distributed (21 nodes radially by 9 axially) over the gage length section, Fig. 2. Starting from standard initial conditions, the boundary conditions are:

$$r=0:\ u=0,\ \frac{\partial p}{\partial r}=0,\ \frac{\partial T}{\partial r}=0$$

$$r=0.635cm:\ p=1atm,\ \frac{\partial T}{\partial r}=0$$

$$z=0:\ w=0,\ \frac{\partial p}{\partial z}=0,\ \frac{\partial T}{\partial z}=0 \qquad (11)$$

$$z=2.54cm:\ w=0,\ \frac{\partial p}{\partial z}=0,\ \frac{\partial T}{\partial z}=0$$

where the model is clearly impermeable and insulated in accordance with the test. Heat is generated by a volume flux of 11.4×10^{6} $J/m^{3}s$.

Results for the five models

· model PERM1: Clamped at z = 0 and 2.54 cm, i.e., u = free;

$k_{virg}=0.465\times10^{-22}m^{2}$, a = 7, ϕ_{openv}= 0.004

· model PERM2: Clamped at z = 0 and 2.54 cm, i.e., u = free;

$k_{virg}=0.930\times10^{-22}m^{2}$, a = 7, ϕ_{openv}= 0.004

· model PERM3: Clamped at z = 0 and 2.54 cm, i.e., u = free;

$k_{virg}=1.860\times10^{-22}m^{2}$, a = 7, ϕ_{openv}= 0.004

· model BIOT1: Clamped at z = 0 and 2.54 cm, i.e., u = free;

$k_{virg}=0.930\times10^{-22}m^{2}$, a = 5, ϕ_{openv}= 0.004

· model BIOT2: Clamped at z = 0 and 2.54 cm, i.e., u = free;

$k_{virg}=0.930\times10^{-22}m^{2}$, a = 9, ϕ_{openv}= 0.004

are presented because for the permeability and a distributions over the porosity, after setting the open virgin and char-state permeabilities, a is chosen to achieve a best fit to the data (Figs. 3, 4, 5 and 6) such that $0<\alpha<1$; for isotropic material, α = 1 means the bulk modulus of the porous material is ni compared to that of the pure <nonporous> solid (Nur and Byerlee[11]).

They closely fit the experimental data as shown in Figs. 3, 4, 5 and 6 in comparison with experimental data. Nonetheless the curve-fitting, established by trial and error comparisons with the test data, is a tedious task and the curves in Figs. 3, 4, 5 and 6 are the outcome of many simulations.

It is found that permeability is the most critical factor controlling material behavior. This is followed by Biots constants. Our results settle upon an open porosity in virgin material five times less than the actual porosity. Furthermore, the following controlling factors emerge:

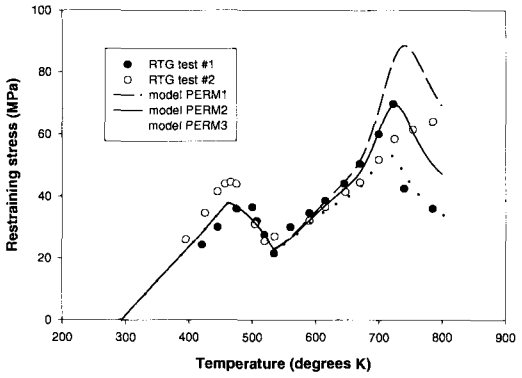

Fig. 3. RTG restraining stress vs. temperature for constant coefficient of porosity a

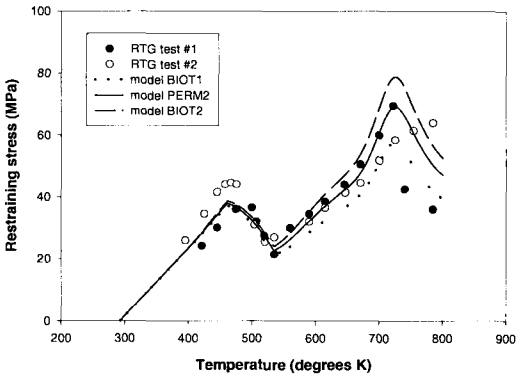

Fig. 4. RTG restraining stress vs. temperature for constant permeability at char-state

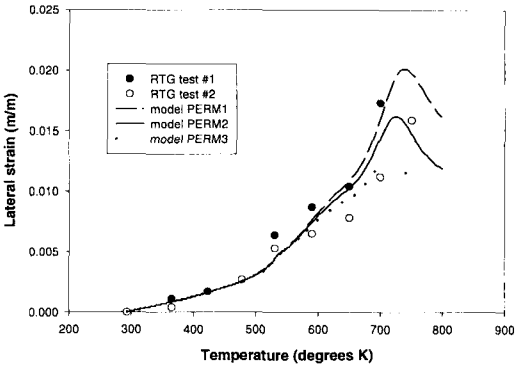

Fig. 5. RTG lateral strain versus temperature for constant coefficient of porosity

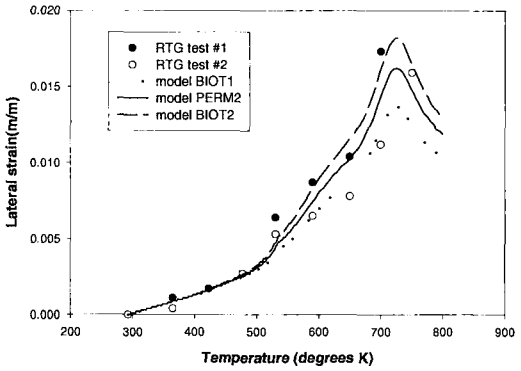

Fig. 6. RTG lateral strain versus temperature for constant permeability at char-state

· The permeability of the virgin material governs the temperature at which the second stress peak occurs as well as its amplitude. The permeability are very small for such a material. The experimental result for the permeability of the virgin material was investigate in range from 10^{-17} to $10^{-22}m^2$ by Stokes[12] who had some difficulty in determining the permeability of the virgin material because it is too low[13]. Some differences can be discerned between the permeability of simulation and test. Because this permeability is a decreasing function of the compressive stress applied on the material and during the RTG test the constraint inside the material goes up to 70MPa[12].

· Lower permeabilities tend to cause higher peaks at higher temperatures. Because lower velocity which results in a lower permeability prevent the pyrolysis gases in pore from escaping out the material and the pyrolysis gases are generated faster than the growth of pore channel can accumulate in flow.

· Biots constants govern the overall

amplitude of the response. Higher factors cause higher response. According to measurements carried out in Fibre ate al. [10], the best fit value for the coefficient of the porosity a for lime stone is a = 4.1 and for sandstone is a = 5.5. The value for RTG simulation is a = 7. This can be caused by the variety of mineralogy, the presence of some microcracks in the sandstone rock [10] and as the increasing rate of open porosity in this study is faster than it is for the actual porosity, it is the same effect that microcracks is increased.

These observations also hold for lateral strain in the specimens. In Figs. 5 and 6, lateral strain is plotted versus temperature for five models along with the measured results from the RTG data. Importantly the Model PERM 2 provides the overall best fit to the data. These results show that the revised theory provides better fits to the experimental data than those by Lee, Salamon and Sullivan[1]

2.8 Free Thermal Expansion Results

Test conditions for the FTE experiment are the same as those for the RTG except that the specimen is 0.635 cm dia. and unconstrained. Likewise, the finite element simulation differs only in geometry and boundary conditions which are:

$$r=0:\ u=0,\ \frac{\partial p}{\partial r}=0,\ \frac{\partial T}{\partial r}=0 \qquad (12)$$

$$r=0.3175cm:\ p=1atm,\ \frac{\partial T}{\partial r}=0$$

$$z=0:\ w=0,\ p=1atm,\ \frac{\partial p}{\partial z}=0,\ \frac{\partial T}{\partial z}=0$$

$$z=2.54cm:\ \frac{\partial p}{\partial z}=0,\ \frac{\partial T}{\partial z}=0$$

so that the FTE specimen is subject to atmospheric pressure, but thermally insulated. These are applied to a model of 200 axisymmetric, quadrilateral finite elements (11 nodes radially by 21 axially) over the gage length section (Fig. 2).

The results shown in Fig. 7 and 8 are for five material models which have same permeability as model PERM 2 of RTG:

· model FBIOT1:

$k_{virg} = 0.930\times10^{-22}m^2$, a = 7, ϕ_{openv}= 0.004

· model FBIOT2:

$k_{virg} = 0.930\times10^{-22}m^2$, a = 13, ϕ_{openv}= 0.004

· model FBIOT3:

$k_{virg} = 0.930\times10^{-22}m^2$, a = 19, ϕ_{openv}= 0.004

· model OPEN1:

$k_{virg} = 0.930\times10^{-22}m^2$, a = 13, ϕ_{openv}= 0

· model OPEN2:

$k_{virg} = 0.930\times10^{-22}m^2$, a = 13, ϕ_{openv}= 0.008

The results for the five models presented in Fig. 7 and 8 are the only ones found which provide reasonable fits to the data. They suggest that for free thermal expansion of dry FM5055 material, a is higher than it is for the RTG test. Importantly the model FBIOT 2 provides the best fit to the data.

The value of the Biots constants used in the RTG and FTE simulations are plotted versus porosity of material in Fig. 9. The difference Biots constants in the RTG and FTE simulations are due to the boundary conditions between at the ends of the models fixed and free, respectively, the evolution of pore growth in RTG is slower than it is for the FTE and the pressure of FTE is lower than it is for the RTG. It is concluded that FTE of a specimen provides no mechanical mechanism to promote coalescence of pores and growth of a porous network or the generation of new pores.

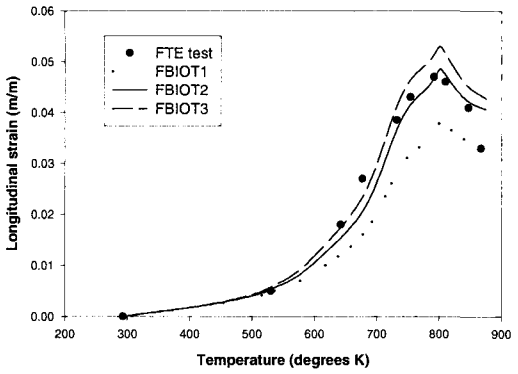

Fig. 7. FTE longitudinal strain versus temperature for constant permeability

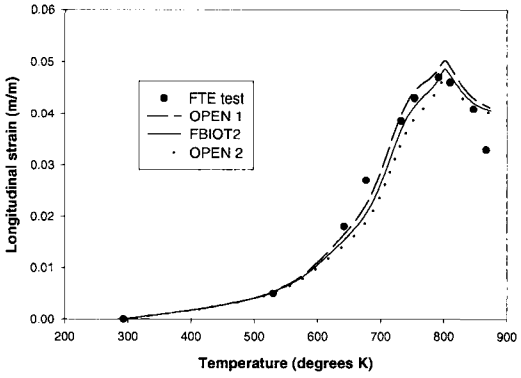

Fig. 8. FTE longitudinal strain versus temperature for constant porosity a

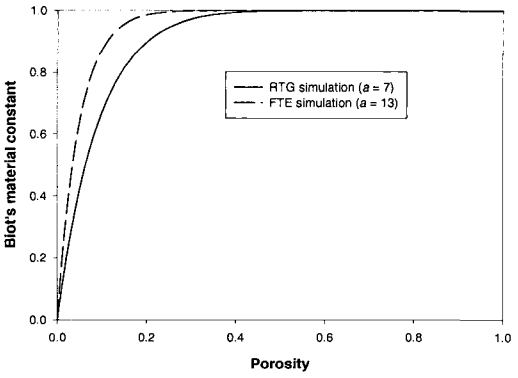

Fig. 9. Biots constants versus porosity for using the model RTG and FTE simulation (best fit)

3. CONCLUSION

A revised axisymmetric theory applied to FM5055 carbon-phenolic insulation material using a modified finite element program strongly suggests that the test specimens had very low permeability, about $0.930\times10^{-22}m^2$ in virgin material, which falls at the low end of a range of permeability measurements. Simulations of restrained thermal growth experiments further reveal how the Biots constants and permeability affect the behavior of the material under increasing temperature; the Biots constants affects overall response, the permeability plays a stronger local role by controlling location, amplitude and sharpness of pore pressure peaks and lower permeabilities tend to cause higher peaks at higher temperatures.

Simulation of free thermal expansion experiments further support the above conclusion that permeability and Biots constants affect the behavior of the material. But FTE simulations required higher Biots constants to fit the data than it is for RTG simulation and the evolution of pore growth in RTG is slower than it is for the FTE. Even then reveal a especially strong sensitivity to both parameters of the permeability and Biots constants.

References

[1] Lee, S., Salamon, N.J. and Sullivan, R.M., 1996, Finite Element Analysis of Poroelastic Composites Undergoing Thermal and Gas Diffusion , J. of Thermophysics and Heat Transfer, Vol. 10, No. 4, pp. 672-680.

[2] Sullivan, R.M. and Salamon, N.J., 1992a, A

Finite Element Method for the Thermochemical Decomposition of Polymeric Materials-Part I : Theory, International Journal of Engineering Science, Vol. 30, No. 4, pp. 431-441.

[3] Sullivan, R.M. and Salamon, N.J., 1992b, A Finite Element Method for the Thermochemical Decomposition of Polymeric Materials-Part I: Carbon Phenolic Composites, ibid, No. 7, pp. 939-951.

[4] Weiler, F.C., 1992, Fully Coupled Thermo-Poro-Elasto Governing Equations, in Computational Mechanics of Porous Materials and Their Thermal Decomposition, N.J. Salamon and R.M. Sullivan, Edts., AMD-Vol. 136, ASME Press.

[5] Wu, Yinan and Katsube, Noriko, 1996, A Constitutive Model for Thermomechanical Response of Decomposing Composites Under High Heating Rates , Mechanics of Materials, Vol. 22, pp. 189-201.

[6] Stokes, E.H., 1987, The Effect of Moisture on the Mechanical and Thermal Response of FM5055 Carbon Phenolic Composites, Southern Research Institute Report No. SRI-EAS-87-1244-6245-6, Southern Research Institute, Birmingham, AL.

[7] Biot, M.A., 1941, General Theory of Three-Dimensional Consolidation, Journal of Applied Physics, Vol. 12., February, pp. 155-164.

[8] Lee, Sunpyo, 1993, Coupled Finite Element Analysis of Decomposing Polymeric Composites and Structures with Subsequent Thermal and Gas Diffusion, Ph.D. Dissertation, The Pennsylvania State University.

[9] Ganesan, Ramnath, 1996, Fundamental Modeling Studies of the Thermal-Mechanical Response of Decomposing Polymers , Ph.D. Dissertation, The Pennsylvania State University.

[10] Fabre, Denis and Gustkiewicz, Jerzy, 1998, Influence of rock porosity on Biots coefficient, Poromechanics A Tribute to Maurice A. Biot, A.A.BALKEMA/ ROTTERDAM/ BROOKFIELD Press.

[11] Nur, A. and Byerlee, J.D., 1971, An Exact Effective Stress Law for Elastic Deformation of Rock with Fluids, Journal of Geophysical Research, Vol. 76, No. 26, pp. 6414-6419.

[12] E. H. Stokes, 1992, Permeability of Carbonized Rayon based Polymer Composite, Computational Mechanics of Porous Materials and Their Thermal Decomposition ASME, AMD-VOL. 136, pp. 145-156

[13] Sullivan, R.M., 1990, A Finite Element Model for Themochemically Decomposing Polymers, Ph.D. Dissertation, The Pennsylvania State University.

Appendix

· Mechanical properties

Temperature Range	$E_L(Pa)$	$E_T(Pa)$
T<293K	1.517×10^{10}	1.793×10^{10}
293K<T<460K	$-1.269\times10^{7}T+1.889\times10^{10}$	$-1.383\times10^{7}T+2.198\times10^{10}$
460K<T<533K	$-1.199\times10^{8}T+6.819\times10^{10}$	$-1.433\times10^{8}T+8.513\times10^{10}$
533K<T<790K	$-1.308\times10^{7}T+1.127\times10^{10}$	5.160×10^{9}
T>790K	9.383×10^{8}	5.160×10^{9}

Temperature Range	Property	Value
T<293K	ν_{TL}	0.30
	ν_{LT}	0.22
	ν_{T}	0.20
293K<T<460K	ν_{TL}	0.30
	ν_{LT}	0.22
	ν_{T}	0.20
460K<T<533K	ν_{TL}	$-4.108\times10^{-3}T+2.190$
	ν_{LT}	$-1.507\times10^{-3}T+0.913$
	ν_{T}	$-2.793\times10^{-3}T+1.460$
533K<T<790K	ν_{TL}	0
	ν_{LT}	$-4.280\times10^{-4}T+0.3381$
	ν_{T}	0
T>790K	ν_{TL}	0
	ν_{LT}	0
	ν_{T}	0

· Material properties

Property	Value
β_T	0.00000833 m/mK
β_L	0.00001607 m/mK
ϕ_{virg}	0.02
ϕ_{char}	0.19
ρ_{virg}	1500.0 kg/m
ρ_{char}	1400.0 kg/m
$(C_p)_{solid}$	1338.0 J/kgK
$(C_p)_{gas}$	1088.0 J/kgK
χ_{solid}	1.44 $J/m\sec K$
χ_{gas}	0.0 $J/m\sec K$